

Generation of triangular-shaped optical pulses in normally dispersive fibre

This article has been downloaded from IOPscience. Please scroll down to see the full text article.

2010 J. Opt. 12 035205

(<http://iopscience.iop.org/2040-8986/12/3/035205>)

View [the table of contents for this issue](#), or go to the [journal homepage](#) for more

Download details:

IP Address: 134.151.33.144

The article was downloaded on 20/04/2010 at 13:12

Please note that [terms and conditions apply](#).

Generation of triangular-shaped optical pulses in normally dispersive fibre

Hua Wang^{1,2}, Anton I Latkin³, Sonia Boscolo¹, Paul Harper¹ and Sergei K Turitsyn¹

¹ Photonics Research Group, School of Engineering and Applied Science, Aston University, Birmingham B4 7ET, UK

² Institute of Physics, Nankai University, 300071 Tianjin, People's Republic of China

³ Novosibirsk State University, Pirogova street 2, 630090 Novosibirsk, Russia

E-mail: wangh9@aston.ac.uk, latkin@gmail.com, s.a.boscolo@aston.ac.uk, p.harper@aston.ac.uk and s.k.turitsyn@aston.ac.uk

Received 14 October 2009, accepted for publication 16 December 2009

Published 1 February 2010

Online at stacks.iop.org/JOpt/12/035205

Abstract

We determine through numerical modelling the conditions for the generation of triangular-shaped optical pulses in a nonlinear, normally dispersive (ND) fibre and experimentally demonstrate triangular pulse formation in conventional ND fibre.

Keywords: nonlinear pulse shaping, nonlinear optical fibre, triangular pulses

(Some figures in this article are in colour only in the electronic version)

1. Introduction

Controlling the shape of optical pulses has become increasingly important for many scientific applications, including ones in ultra-high-speed optical systems, quantum optics, and nonlinear optics. The possibility of changing the pulse waveform from the well known Gaussian and hyperbolic secant shapes to more exotic parabolic or triangular pulses could be of use for various applications in optical signal processing and manipulation. In [1], transform-limited pulse shapes were generated by temporal coherent synthesis using a multi-arm interferometer. Generation of pulses with flat-top [2], parabolic [3, 4] and sawtooth (asymmetric triangular) [5] shapes has been demonstrated using superstructured fibre Bragg grating (FBG) technology. A flat-top pulse generator approach based on an FBG in transmission has been presented in [6]. Flat-top, parabolic and triangular pulses can also be produced through the use of nonlinear effects in optical fibres. Recently, we have introduced a method for passive nonlinear pulse shaping in the time domain, which relies on a combination of pulse pre-chirping (the chirp being the first time derivative of the phase) and nonlinear propagation in a section of normally dispersive (ND) fibre [7]. Such recent advances in pulse shaping have paved the way for transferring several techniques of signal manipulation well developed in electronics to the optical domain.

The simple intensity profile of triangular pulses is highly desired for a range of photonic applications. For instance, sawtooth pulses have been shown to enhance the performance of wavelength converters based on self-phase modulation in fibre and offset filtering [5]. Time-domain add-drop multiplexing based on cross-phase-modulation (XPM)-induced frequency shifting in fibre using sawtooth control pulses was examined in [8]. A novel technique of copying optical pulses in both the frequency and time domains based on a combination of XPM with a triangular pump pulse in a nonlinear Kerr medium and subsequent propagation in a dispersive medium was introduced in [9]. The usage of XPM with a triangular pump pulse train for realizing time-to-frequency mapping of multiplexed signals in high-speed fibre communication systems was theoretically investigated in [10]. In this paper, we present results of numerical modelling which determine the parameters required for the generation of triangular-shaped optical pulses in a nonlinear ND fibre. We also present experimental evidence of triangular pulse shaping in conventional ND fibre.

2. Triangular pulse shaping

In the passive pulse shaping scheme introduced in [7], Kerr nonlinearity and group-velocity dispersion (GVD) in a ND fibre lead to various reshaping processes of an initial,

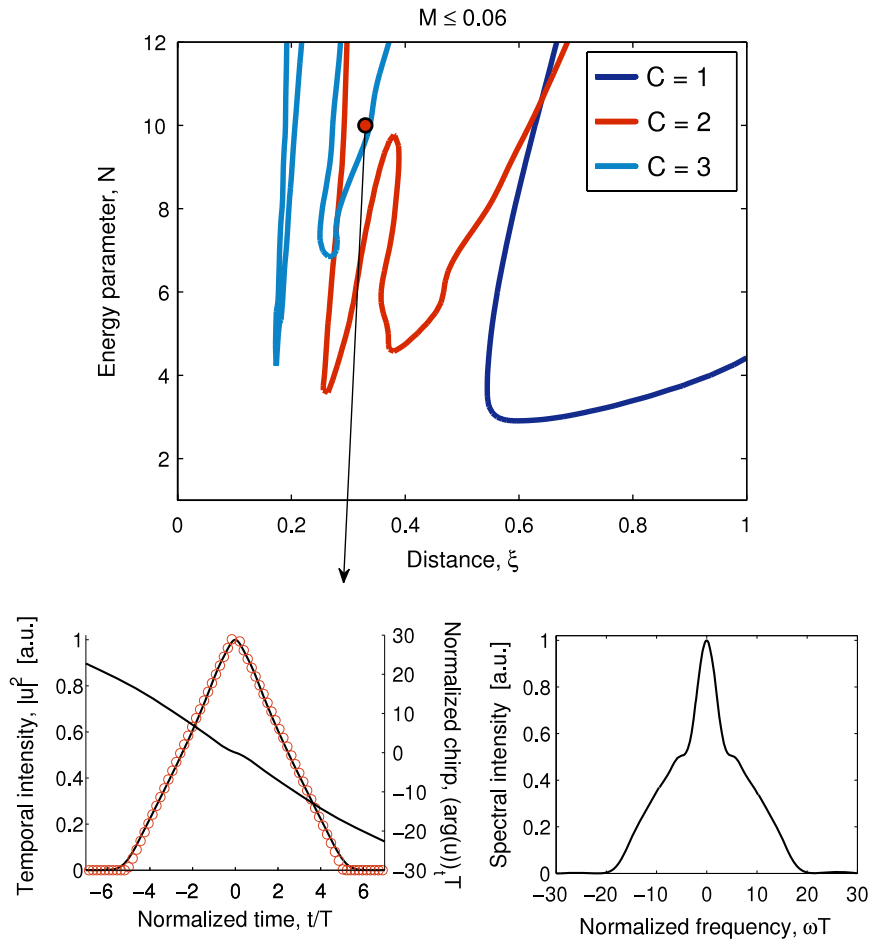


Figure 1. Contours of the misfit parameter $M \leq 0.06$ in the energy parameter–distance plane. Inset: sample pulse temporal and spectral characteristics. Circles: triangular fit.

conventional pulse according to the chirping value and power level at the input of the fibre. Control of the pulse chirp and power at the fibre input is realized through the use of a pre-chirping device and an optical amplifier, respectively. In particular, we have observed that triangular-shaped pulses can be generated for sufficiently high energies and a positive initial chirp parameter (using the definition $iC'T^2$ for the phase profile). For the purpose of illustration, here we consider a Gaussian-shaped pulse as the pulse input to the ND fibre. Note that for a different choice of the initial pulse shape, pulse reshaping processes similar to those illustrated in this paper are expected to occur upon propagation in a ND fibre, whereas the relevant parameter regions would be different [12]. Pulse propagation in the fibre is numerically modelled using the standard nonlinear Schrödinger equation [11].

Figure 1 shows the processes of pulse reshaping to a nearly ideal triangular intensity profile that can take place in the fibre for different values of the normalized chirp parameter $C = C'T^2$. There, we used the parameter of misfit, M [4], between the pulse intensity profile and a triangular fit of the same energy and full width at half-maximum (FWHM) duration:

$$M^2 = \frac{\int dt (|u|^2 - |u_T|^2)^2}{\int dt |u|^4}$$

to define regions of triangular pulse formation in the plane of energy parameter ('soliton' number) $N = (T^2\gamma P_0/\beta_2)^{1/2}$ (ranging from 1 to 12) against normalized distance $\xi = \beta_2 z/T^2$ (from 0 to 1). Here, $u(z, t)$ is the pulse envelope in the comoving system of coordinates, $u_T(t)$ corresponds to the intensity profile $|u_T(t)|^2 = P_{0,T}(1 - |t/\tau|)\theta(\tau - |t|)$ with $\theta(x)$ being the Heaviside function, T and P_0 are respectively a characteristic temporal width (e.g., the half-width at the 1/e of intensity point in the case of a Gaussian-shaped pulse) and the peak power of the initial pulse, and β_2 and γ are the respective GVD and nonlinearity parameters of the fibre. The triangular pulse regions in figure 1 are defined by contours of the misfit parameter M less than or equal to a sufficiently small value, which is set to 0.06 as an example. A typical example of shaped pulse temporal and spectral intensity profiles and of the corresponding chirp profile is shown in the inset of figure 1. In this example, $C = 2$, $N = 10$, $\xi = 0.33$, and parameter M is as low as 0.03. The triangular temporal fit is also plotted, showing very good agreement with the actual pulse shape. It is also seen that the chirp is highly linear across the entire pulse duration. This is an additional attractive feature of the triangular pulses generated for all-optical signal processing applications.

Note that the use of dimensionless quantities in our analysis enables us to obtain results that can be applied in

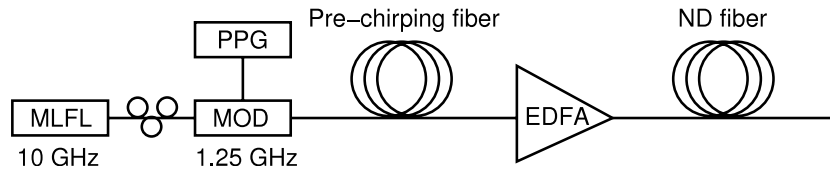


Figure 2. Experimental set-up for triangular pulse generation.

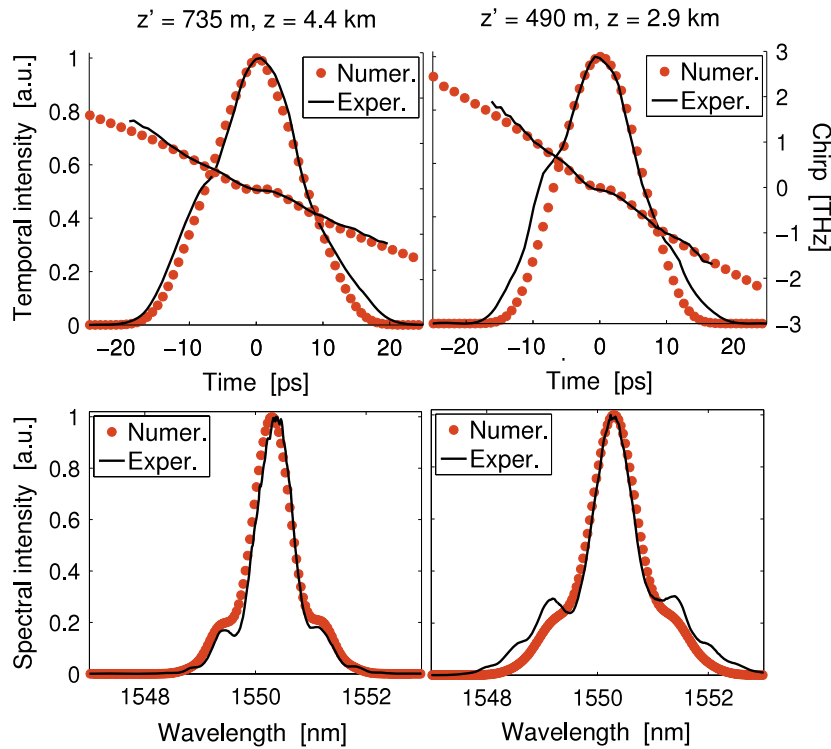


Figure 3. Experimental (solid lines) and numerical (circles) pulse temporal intensity and chirp profiles and spectra at the TWF output. Left, pre-chirping fibre length $z' = 735$ m and TWF length $z = 4.4$ km. Right, $z' = 490$ m and $z = 2.9$ km.

a variety of situations in real world units by scaling of the relevant quantities. A target pulse shape (triangular here) can be achieved by changing C , N and ξ . In practical situations, it is usually the case that one has a transform-limited pulse source with a given pulse duration T_0 , and a length z of ND fibre with given dispersive and nonlinear characteristics, β_2 and γ . Pulse pre-chirping can be conveniently realized by propagating the source pulse through a length z' of linear, dispersive fibre. This will impose a chirp parameter C' as well as a duration T on the pulse at the input of the ND fibre. For instance, in the case of a Gaussian pulse, C' and T read $C' = -\beta_2' z' / [2T_0^4 (1 + (\beta_2' z' / T_0^2)^2)]$ and $T = T_0 \sqrt{1 + (\beta_2' z' / T_0^2)^2}$, with β_2' being the GVD parameter of the pre-chirping fibre. Figure 1 can be then read as follows: it says whether a triangular pulse intensity profile can be observed at the output z of the ND fibre, and in which value range the input peak power P_0 should be chosen for different selected values of the input chirp parameter C' .

We also note that here we only consider pulses in the picosecond regime. For narrower pulses with higher peak powers other nonlinear mechanisms may play a part in the pulse shaping and higher-order dispersive effects may need to be considered.

3. Experiments

In order to validate our theoretical results, we have carried out the following experimental verification. The experimental set-up is shown schematically in figure 2. The 2.8 ps near transform-limited pulses from a mode-locked fibre laser (MLFL) operating at 1550.3 nm, with a repetition rate of 10 GHz were modulated down to a repetition rate of 1.25 GHz using a lithium niobate Mach-Zehnder modulator. This was so that sufficiently high pulse energies could be achieved at the relatively low saturated output power of the erbium-doped fibre amplifier (EDFA) available for this experiment. The control of the pulse pre-chirping value was realized by propagation through different lengths of standard single-mode fibre (SMF), which had a positive dispersion coefficient $D = -2\pi c\beta_2/\lambda^2 = 16.3$ ps nm⁻¹ km⁻¹ at $\lambda = 1550.0$ nm, which imposed a positive chirp parameter C' on the pulse. The pre-chirped pulses were amplified to different power levels using an EDFA, and then propagated through a ND fibre to realize the pulse reshaping. In our experiment, ‘TrueWave’ fibre (TWF) was used as the ND fibre. The dispersion coefficient of this fibre was $D = -3.104$ ps nm⁻¹ km⁻¹ at $\lambda = 1550.0$ nm,

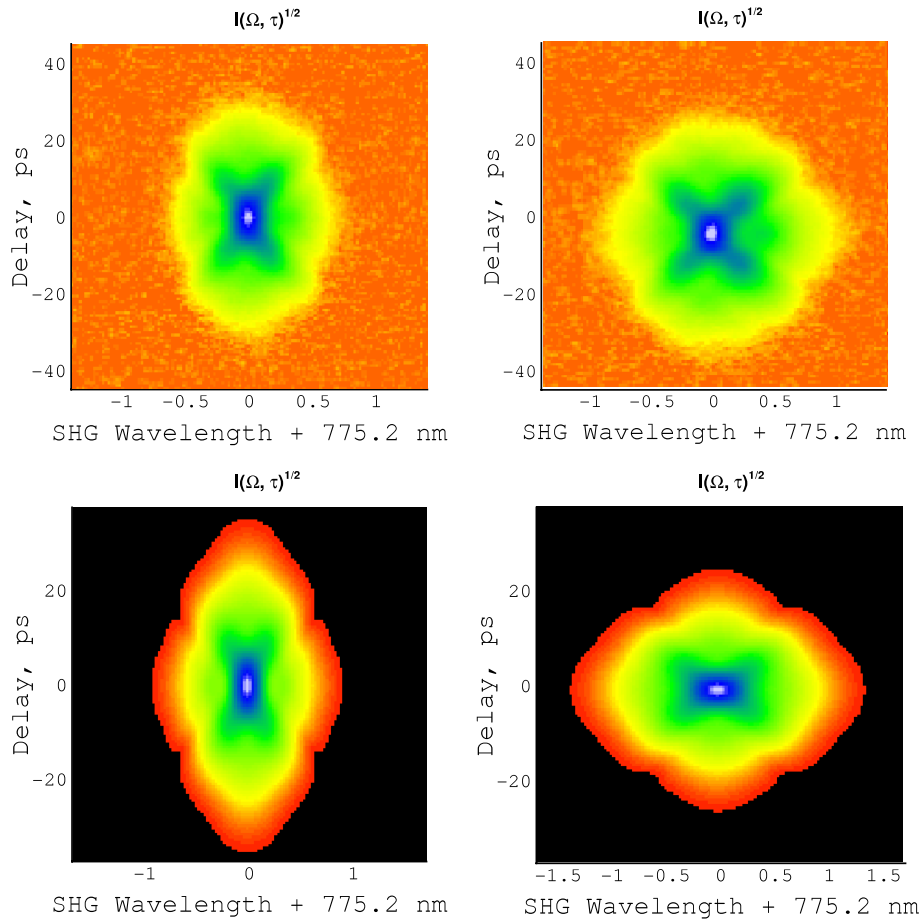


Figure 4. Experimental (top) and theoretical (bottom) SHG-FROG spectrograms of the pulses in figure 3 for pre-chirping fibre lengths $z = 4.4$ km (left) and $z = 2.9$ km (right).

nonlinear coefficient $\gamma \approx 2.5 \text{ W}^{-1} \text{ km}^{-1}$, and dispersion slope $dD/d\lambda = 0.0669 \text{ ps nm}^{-2} \text{ km}^{-1}$. The output pulses from the TWF were characterized using a second-harmonic-generation frequency resolved optical gating (SHG-FROG) [13]. The spectrograms from the SHG-FROG were then processed to retrieve the temporal and phase characteristics of the output pulses. The output pulse spectra were also measured using an optical spectrum analyzer (OSA). For different chirp parameters, the TWF length was altered to give the best triangular pulse output.

Figure 3 shows the experimental and numerical temporal intensity and chirp profiles retrieved from SHG-FROG spectrograms, and optical spectra of the output pulses from the TWF for two different lengths of pre-chirping fibre, $z' = 735$ m and $z' = 490$ m. The respective TWF lengths were $z = 4.4$ km and $z = 2.9$ km. The effective average launch powers, into the TWF, were 12 dBm in both cases. The corresponding SHG-FROG spectrograms of the experimentally and theoretically generated pulses are depicted in figure 4. It can be seen from figure 3 that the nearly constant gradients of leading and trailing edges, linear chirp profiles and spectral side lobe characteristics of the pulses generated are the distinctive features of the target triangular-shaped optical pulses. There is good qualitative agreement between experiments and numerical simulations. The relevant

dimensionless quantities are $C = 2.7$, $N = 6.5$, $\xi = 0.20$, and $C = 1.8$, $N = 5.3$, $\xi = 0.29$, respectively. These would yield theoretical misfit parameter values of the order of 0.05 according to the estimates that can be made from figure 1. Furthermore, the SHG-FROG spectrograms of the generated pulses in figure 4 are similar to the spectrogram of an ideal theoretical triangular-shaped pulse, which also indicates clearly that good quality triangular-shaped pulses have been generated for both cases.

4. Conclusion

We have demonstrated the possibility of generating triangular intensity pulses by using pulse pre-chirping and progressive pulse reshaping in a nonlinear ND fibre. By choosing the initial chirp and power, and the length of the fibre according to the nature of the pulses, one can expect to have a triangular pulse at the system output. The system design parameters required for triangular pulse formation have been defined in the case of an initial Gaussian pulse. Our theoretical results are confirmed experimentally. The passive nonlinear pulse shaping method discussed here offers thus an attractive and simple way of generating triangular pulses. Such pulses have a range of promising applications in the field of photonics.

Acknowledgments

The research of Hua Wang was supported by the China National Natural Science Foundation (grant 60878010) and the Tianjin Research Plan (contract 08JCYBJC14900).

References

- [1] Park Y, Asghari M H, Ahn T J and Azaña J 2007 Transform-limited picosecond pulse shaping based on temporal coherence synthesization *Opt. Express* **15** 9584–99
- [2] Petropoulos P, Ibsen M, Ellis A D and Richardson D J 2001 Rectangular pulse generation based on pulse reshaping using a superstructured fiber Bragg grating *IEEE J. Lightwave Technol.* **19** 746–52
- [3] Parmigiani F, Petropoulos P, Ibsen M and Richardson D J 2006 Pulse retiming based on XPM using parabolic pulses formed in a fiber Bragg grating *IEEE Photon. Technol. Lett.* **18** 829–31
- [4] Parmigiani F, Finot C, Mukasa K, Ibsen M, Roelens M A F, Petropoulos P and Richardson D J 2006 Ultra-flat SPM-broadened spectra in a highly nonlinear fiber using parabolic pulses formed in a fiber Bragg grating *Opt. Express* **14** 7617–22
- [5] Parmigiani F, Ibsen M, Ng T T, Provost L, Petropoulos P and Richardson D J 2008 An efficient wavelength converter exploiting a grating-based saw-tooth pulse shaper *IEEE Photon. Technol. Lett.* **20** 1461–63
- [6] Preciado M A and Muriel M A 2009 Flat-top pulse generation based on a fiber Bragg grating in transmission *Opt. Lett.* **34** 752–4
- [7] Boscolo S, Latkin A I and Turitsyn S K 2008 Passive nonlinear pulse shaping in normally dispersive fiber systems *IEEE J. Quantum Electron.* **44** 1196–203
- [8] Li J, Olsson B E, Karlsson M and Andrekson P A 2005 OTDM add-drop multiplexer based on XPM-induced wavelength shifting in highly nonlinear fiber *IEEE J. Lightwave Technol.* **23** 2654–61
- [9] Latkin A I, Boscolo S, Bhamber R S and Turitsyn S K 2009 Doubling of optical signals using triangular pulses *J. Opt. Soc. Am. B* **26** 1492–96
- [10] Bhamber R S, Boscolo S, Latkin A I and Turitsyn S K 2008 All-optical TDM to WDM signal conversion and partial regeneration using XPM with triangular pulses *ECOC 2008: Proc. 34th European Conf. on Optical Communication* paper Th.1.B.2
- [11] Agrawal G P 2001 *Nonlinear Fiber Optics* 3rd edn (San Francisco, CA: Academic)
- [12] Finot C, Provost L, Petropoulos P and Richardson D J 2007 Parabolic pulse generation through passive nonlinear pulse reshaping in a normally dispersive two segment fiber device *Opt. Express* **15** 852–64
- [13] Dudley J M, Barry L P, Bollond P G, Harvey J D and Leonhardt R 1998 Characterizing pulse propagation in optical fibers around 1550 nm using frequency-resolved optical gating *Opt. Fiber Technol.* **4** 237–65